Journal of Materials Research

# Lamellar structures in directionally solidified naphthalene suspensions

--Manuscript Draft--

| | |
|---|---|
| **Manuscript Number:** | JMRS-D-23-01288 |
| **Full Title:** | Lamellar structures in directionally solidified naphthalene suspensions |
| **Article Type:** | Article |
| **Section/Category:** | Metal Materials |
| **Funding Information:** | Marshall Space Flight Center (80NSSC18K0196) — Dr David C. Dunand |
| **Abstract:** | To investigate naphthalene as a suspending fluid for freeze-casting applications, sterically stabilized suspensions of copper microparticles suspended in liquid naphthalene are directionally solidified in a Bridgman furnace. Colonies of nearly particle-free naphthalene lamellae, interspersed with particle-enriched interlamellar regions, are predominantly aligned in the direction of the imposed thermal gradient. As furnace translation velocities decrease from 80 to 38 to 6.5 μm · s−1, the naphthalene lamellae become thicker. For the lowest velocity, a transition to a lensing microstructure (with naphthalene bands aligned perpendicular to the solidification direction) is observed in central regions of samples. For all velocities, the naphthalene lamellae show (i) secondary dendritic arms on one of their sides and (ii) are thinnest within core regions relative to peripheral regions (closest to the ampoule walls). Together, these observations suggest the presence of buoyancy-driven convection during solidification. |
| **Corresponding Author:** | Kristen Scotti<br>Northwestern University Department of Materials Science and Engineering<br>Evanston, IL - Illinois UNITED STATES |
| **Corresponding Author Secondary Information:** | |
| **Corresponding Author's Institution:** | Northwestern University Department of Materials Science and Engineering |
| **Corresponding Author's Secondary Institution:** | |
| **First Author:** | Kristen Scotti |
| **First Author Secondary Information:** | |
| **Order of Authors:** | Kristen Scotti |
| | Peter W. Voorhees |
| | David C. Dunand |
| **Order of Authors Secondary Information:** | |
| **Author Comments:** | |
| **Suggested Reviewers:** | Grae Worster<br>University of Cambridge Department of Applied Mathematics and Theoretical Physics<br>mgw1@cam.ac.uk<br>Knowledge of freeze-casting and author of model compared in text |
| | Sylvain Deville<br>Institut Lumière Matière: Institut Lumiere Matiere<br>sdeville@gmail.com<br>Extensive knowledge of the freeze-casting technique |
| | Ulrike Wegst<br>Dartmouth College<br>urlike.wegst@dartmouth.edu<br>Extensive knowledge of the freeze-casting technique |
| | |

| | |
|---|---|
| | Zhijun Wang<br>State Key Laboratory of Robotics: Shenyang Institute of Automation Chinese Academy of Sciences<br>zhjwang@nwpu.edu.cn<br>Knowledge of the freeze-casting technique |
| | Xin Lin<br>State Key Laboratory of Robotics: Shenyang Institute of Automation Chinese Academy of Sciences<br>xlin@nwpu.edu.cn<br>Knowledge of the freeze-casting technique |

# Lamellar structures in directionally solidified naphthalene suspensions

*Kristen L. Scotti*[1*], *Peter W. Voorhees*[1], *and David C. Dunand*[1]

[1]Department of Materials Science and Engineering, Northwestern University, Evanston, IL 60208, USA

## Abstract

To investigate naphthalene as a suspending fluid for freeze-casting applications, sterically-stabilized suspensions of copper microparticles suspended in liquid naphthalene are directionally solidified in a Bridgman furnace. Colonies of nearly particle-free naphthalene lamellae, interspersed with particle-enriched interlamellar regions, are predominantly aligned in the direction of the imposed thermal gradient. As furnace translation velocities decrease from 80 to 38 to 6.5 $\mu m \cdot s^{-1}$, the naphthalene lamellae become thicker. For the lowest velocity, a transition to a lensing microstructure (with naphthalene bands aligned perpendicular to the solidification direction) is observed in central regions of samples. For all velocities, the naphthalene lamellae show (i) secondary dendritic arms on one of their sides and (ii) are thinnest within core regions relative to peripheral regions (closest to the ampoule walls). Together, these observations suggest the presence of buoyancy-driven convection during solidification.

**Keywords:** freeze-casting, ice lenses, porous metals, convection, Bridgman

## 1. Introduction

Directional freeze-casting [1-3] is a solidification technique that is used to create anisotropic porous metallic [4], ceramic [5], and polymeric [6] materials. For metallic and ceramic material processing, the process typically involves solidification of particle suspensions under the presence of a thermal gradient. As solidification progresses, the suspension fluid solidifies into

* Corresponding author. Tel.: +1 331 425 4979
E-mail address: kristenscotti@u.northwestern.edu (K.L. Scotti)

dendrites/plates which reject the suspended particles and grow along the direction of the induced thermal gradient, while particles are incorporated within interdendritic/interlamellar space. A porous structure is obtained by removal of the solidified, particle-depleted fluid *via* sublimation. For metals and ceramics, particle-packed walls are then sintered to form a solid matrix [1, 2].

As pores are templated by the morphology of the solidified particle-depleted fluid, the pore shape of freeze-cast materials is largely determined by the choice of suspending fluid [1, 2]. Aqueous suspensions are most often employed, resulting in a range of lamellar [7] to dendritic pore structures [8]. Camphene [9] and tert-butyl alcohol [10] result in highly dendritic and elongated tubular structures, respectively. In a camphor-naphthalene fluid system [11-13], the pore structure can be adjusted by changing the composition of the fluid mixture, *i.e.*, from dendrites, to rods, to plates for hypoeutectic, eutectic, and hypereutectic compositions of camphor-naphthalene, respectively [13]. However, the microstructure images accompanying these reports show that pores do not appear homogeneously aligned throughout these samples [11-13].

Here, we utilize only naphthalene (an apolar polycyclic aromatic hydrocarbon) as the freeze-casting suspending fluid; naphthalene/Cu particle suspensions are sterically stabilized and directionally solidified to characterize the corresponding microstructure. As naphthalene solidifies with faceted interfaces [14], it should yield anisotropic pore structures when employed as a freeze-casting suspension fluid. The relatively high melting temperature of naphthalene (80°C [15]) and vapor pressure (130 Pa at 52°C [11]) allows for sublimation at room temperature/ambient pressure, as reported elsewhere [11-13]. Here, we investigate the as-solidified microstructure to better correlate processing conditions to microstructural characteristics, because post-solidification processing steps, which result in anisotropic shrinkage during sublimation [16] and sintering [17], often obscure these processing-structure connections.

## 2. Experimental methods

### 2.1. Specimen preparation

As received naphthalene ($C_{10}H_8$, 99.6% purity, Sigma Aldrich, St. Louis, MO, USA) was first vacuum-distilled at ~90°C. Due to the relatively high solubility of atmospheric gases in liquid naphthalene [18-22], suspensions were prepared under helium atmosphere using a Schlenk line. The polymeric surfactant Hypermer KD-13 (Croda Inc., Edison, NJ, USA) was incorporated at a concentration of 1 wt.% (with respect to intended Cu mass) into the distilled naphthalene and equilibrated *via* stirring for ~12 h at ~90°C. Copper microparticles (1 μm, SkySpring Nanomaterials, Inc, Houston, TX, USA), which were first dried for 12 h under vacuum at ~100°C to remove moisture adsorbed on their surfaces, were then added to naphthalene/dispersant solutions at a volume fraction of 5% (corresponding to a Cu particle weight fraction of 32%). These suspensions were stirred for 12 h at ~90°C and sonicated for 2 h in a ~90°C water bath. Suspensions were prepared at volumes of either 50 or 100 mL (with equilibration times remaining the same regardless of volume).

Particle suspensions were transferred to quartz ampoules (10 mm inner diameter, ~20 cm in length), placed in a Bridgman furnace (preheated to ~130ºC), and directionally solidified under a constant thermal gradient of $35°C \cdot cm^{-1}$; the furnace was translated vertically upward to achieve upward solidification in the stationary ampoule, with translation velocities, $V$ = 6.5, 38, and 80 $\mu m \cdot s^{-1}$.

### 2.2. Microstructural investigation

Directionally solidified samples were mounted in epoxy, polished, and imaged using a Wild M3Z Stereoscope. Naphthalene lamellae thickness was measured using ImageJ/Fiji [23] from stitched cross-section images taken perpendicular to the freezing direction. These measurements were regionalized using guides: “outer” measurements were taken from a circle

drawn at the periphery of cross-sections and "inner" measurements taken from a circle drawn at the center of cross-sections having a diameter of ~2.5 mm. "Outer-middle" and "middle-inner" measurements were taken from equally spaced circles drawn between the outer and inner circles (thus, distance between any given circle is ~1.25 mm as the sample diameters are ~10 mm). Only lamellae crossing drawn guides were measured. Nine samples were analyzed (three samples for each furnace translation velocity) with 500 measurements taken for each region (at each velocity).

## 3. Results and Discussion

### 3.1. Suspension stability

Naphthalene/Cu particle suspensions (5 vol.% Cu particles, corresponding to 32 wt.% in suspension) were sterically stabilized using 1 wt.% Hypermer KD-13 dispersant with respect to Cu particle mass (0.5 wt.% with respect to naphthalene mass) and suspension stability was assessed by measuring the height of macroscopic particle-depleted regions in solidified samples. As samples are solidified vertically upward, particle sedimentation in the liquid results in particle-enriched and particle-depleted regions; in the solidified samples, the particle-enriched regions begin at the bottom of the samples (first-to-solidify regions) and particle-depletion regions end at the top (last-to-solidify regions). These regions present as a color change in the solidified samples, with particle-enriched regions appearing darker due to the dark color of Cu particles relative to naphthalene, and particle depletion regions presenting as light orange to nearly clear (practically devoid of particles).

Fig. 1 shows the average measured height of the particle depletion regions as percentages of the total solidified sample height (~20 cm) for samples solidified using furnace translation velocities of 6.5, 38, and 80 μm/s. Samples solidified at the highest furnace translation velocity ($V = 80\ \mu m \cdot s^{-1}$) show particle depletion region heights that correspond to 30±7% of the total sample height. Particle depletion region height increases nearly double to 58±15% for samples solidified

using the slowest translation velocity ($V = 6.5\ \mu m \cdot s^{-1}$), where longer solidification times promote increased particle sedimentation. The Stokes' sedimentation velocity for 1 μm Cu particles in liquid naphthalene is ~2.7 $\mu m \cdot s^{-1}$; this corresponds to a particle depletion region comprising ~3, 7, and 42% of sample heights for samples solidified at 80, 38, and 6.5 $\mu m \cdot s^{-1}$, respectively, well below the values reported in Fig. 1. Suspensions containing 0.1 and 2.5 wt.% dispersant (with respect to Cu mass) were produced to assess whether the sedimentation rates could be reduced by modifying dispersant concentration; as the resulting suspensions showed extensive particle sedimentation immediately after preparation, they were not tested further.

### 3.2. Solidified microstructures

Fig. 2 and Fig. 3 show optical micrographs of solidified structures obtained by directionally solidifying the Cu particle suspensions using furnace translation velocities of $V = 80$ and 38 $\mu m \cdot s^{-1}$, respectively. In these images, transparent naphthalene appears black, whereas Cu particles appear golden. Fig. 2 (a) and Fig. 3(a) are taken perpendicular to the freezing direction (the freezing direction is out-of-the-page) and images in Fig. 2 (b) and Fig. 3 (b) are taken parallel to the freezing direction (shown by the white arrow). For both translation velocities, naphthalene is lamellar (or plate-like) with dendritic features (*i.e.*, minor secondary arm growth of naphthalene, resulting in relatively small protrusions on particle-packed walls [7]), some of which are highlighted using small white arrows in Fig. 2-a and Fig. 3-a. The observation of highly anisotropic structures is consistent with facetted growth [24]; *i.e.*, relatively high interfacial anisotropy of the solidifying solid. Microstructural directionality with respect to the imposed thermal gradient (white arrows in Fig. 2-b and Fig. 3-b) is largely retained over the height of these samples.

Preliminary directional solidification tests of Cu particle/naphthalene suspensions were conducted using a typical directional freeze-casting set-up [1], wherein a Teflon mold containing

the suspension was temperature controlled at the top and bottom faces, defining the macroscopic thermal gradient in the solidifying sample, but not the thermal gradient within the interfacial region, specifically. Microstructures similar to those reported in the literature for the camphor-naphthalene fluid system [11-13] were obtained: some local, directional growth of naphthalene was observed, but directionality was not retained over the solidification height for these samples. Fabietti *et al*. [25, 26] reported that instability mechanisms during directional solidification of naphthalene are strongly dependent on the orientation of the solid/liquid interface (which can be influenced by a lack of control over the thermal gradient at the interface [27, 28]). The improved microstructural directionality shown here was obtained only by using a Bridgman furnace. While use of the Bridgman furnace provides better control over the thermal gradient at the solid/liquid interface (thus, may have improved directionality by itself [27, 28]), it also necessitated use of increased sample heights (~20 cm *vs*. 5-15 mm in refs. [11-13] and ~10 mm in our initial studies that used a typical freeze-casting set-up). Grains that are initially misaligned with respect to the thermal gradient will typically rotate such that the preferred crystallographic growth direction is aligned with the thermal gradient; how fast this occurs is dependent on factors such as pulling velocity, thermal gradient, and crystal anisotropy [27]. Thus, the use of increased solidification heights may have contributed to the improved directionality observed here as misoriented grains were provided a longer length scale for orientation corrections.

As noted above, the images in Fig. 2 and Fig. 3 show evidence of secondary arm growth of naphthalene (small white arrows in Fig. 2-a and Fig. 3-a), but the resulting particle-wall protrusions are primarily observed on only one side of particle walls. Asymmetric dendritic features on lamellae, often referred to as “one-sided dendrites” [7], can be promoted due to the presence of interdendritic convective flow during solidification. Similar asymmetric dendritic

features were reported in our previous investigation of aqueous $TiO_2$ suspensions [29]. There, it was proposed that rotating fluid cells between lamellae were promoted due to a shear flow existing at the solid/liquid interface, and the interaction between these fluid flow regimes promoted growth of secondary arms on the upstream side (where heat is more easily transported away from lamellae *via* the fluid flow) while the warmer fluid on the downstream side promoted melting and fragmentation of secondary arms [30]. A similar mechanism can be invoked to explain the asymmetric dendritic features observed in Fig. 2-a and Fig. 3-a.

Fig. 4 shows optical micrographs of solidified structures obtained by directionally solidifying the suspensions at a translation velocity, at $V = 6.5\ \mu m \cdot s^{-1}$. Cross-sections Fig. 4(a) and Fig. 4 (b), are taken perpendicular to the freezing direction, and the images in Fig. 4(c) and (d) are taken parallel to the freezing direction (shown by large white arrows). Cross-sections Fig. 4 (a) and (c) are taken from the outer region of the sample (closest to the ampoule wall) and Fig. 4 (b) and (d) are taken from the central region. Increased wall thickness (or wall merging) is observed in Fig. 4 (b) relative to Fig. 4(a), which is suggestive of a microstructural transition from dendrites to banding (bands are naphthalene plates orientated perpendicular to the freezing direction, which are templated into cracks after sublimation [31]; these are best viewed in parallel cross-sections). The left side of the parallel cross-section in Fig. 4 (c) is toward the outer region of the sample; moving towards the right in the image, the width of the particle walls increases (*i.e.*, wall width increases with increasing distance from the ampoule wall). A dramatic increase in wall width is further observed in Fig. 4(d), which represents the central region of the same sample where banding is observed (small white arrows in Fig. 4-d). Fig. 4(d) shows the central region of the same sample where particle wall width has increased dramatically, and banding is observed (small white arrows in Fig. 4).

### 3.3. Radial segregation

Fig. 5 shows box and whisker plots describing thickness of lamellae. Measurements obtained from the "outer" (or peripheral, closest to the ampoule wall) regions of cross-sections are summarized in the leftmost plot, and the rightmost plot summarizes measurements taken from inner/central regions of samples. The minimum and maximum values of boxes represent the first and third quartiles, respectively; medians are shown as horizontal lines inside the boxes, means are represented by black diamonds, and whiskers represent 1.5 times the interquartile range. Numerical values for the data described in Fig. 5 are provided in Table 1.

Naphthalene lamellar thickness is expected to increase with decreasing solidification velocity [7]; taking the furnace translation velocity as roughly equivalent to solidification velocity, this relationship is observed for all regions. For all translation velocities, lamellae are thickest in the outer region of the samples and a decrease in thickness is observed with decreasing distance from the center (*e.g.*, for samples solidified at $V = 6.5\ \mu m \cdot s^{-1}$, lamellae thickness at the outer and inner regions is 74±30 and 36±15 μm, respectively; for $V = 80\ \mu m \cdot s^{-1}$, these values decrease to 45±23 and 19±10 μm, respectively). This trend—increasing lamellar thickness at outer/peripheral regions of samples relative to inner/central regions—indicates that the local solidification velocity is higher in the central region of the sample relative to the outer region, which is suggestive of macroscopic curvature of the interface during solidification and corresponding convective fluid motion [32]. Similar observations were described in our previous study investigating directional solidification of aqueous $TiO_2$ suspensions [29], wherein a macroscopic curvature of the solid/liquid interface was proposed to explain radial variation in particle wall width (dependent on distance from the center) and banding (solidified fluid, separated by particle-packed regions, and oriented perpendicular to the solidification direction) present in the central regions of samples.

Banding was attributed to particle build-up within the central region of the samples, resulting from the interface curvature itself as well as from convective mixing within the bulk liquid, ahead of the solid/liquid interface. Here, suspensions are solidified in the buoyancy-stable configuration for naphthalene (vertically upward, with denser solid naphthalene below and the lighter liquid suspension above); thus, convective fluid motion is likely promoted due to the presence of radial thermal gradients at the solid/liquid interface.

### 3.4. Model comparison

You *et al.* [31] developed a model for predicting freeze-cast microstructures including dendrites and lenses, where lensing includes both banding (solidified fluid oriented perpendicular to the solidification direction) and "spears," (highly interconnected dendrites whose sidearms merge). The boundary between dendritic and lensing is determined by the relationship between two dimensionless parameters, including the Darcy coefficient ($D$), which describes fluid flow through the particle accumulation layer, given by:

$$D = \frac{\mu V T_m}{k \rho L G} \qquad \text{Eq. 1}$$

where $\mu$ is the dynamic viscosity of the suspending fluid, $V$ is the solidification velocity (taken as the furnace translation velocity), $T_m$ is the melting temperature of the pure fluid (80.23°C for naphthalene [33]), $\rho$ is the density of the solid, pure fluid (976.7 kg · m$^3$ for naphthalene [34]), $L$ is the latent heat of fusion of the pure fluid (146 J/g for naphthalene [35]), $G$ is the imposed thermal gradient (here, $G$ = 35°C· cm$^{-1}$), and $k$ is the permeability of the accumulated particle region, given by:

$$k = \frac{r^2 \left(1 - \phi_p\right)^3}{45 \phi_p^2} \qquad \text{Eq. 2}$$

where $r$ is the particle radius (here, $r$ = 0.5 μm) and $\phi_p$ is the volume fraction of particles in the accumulation region, taken as the random close-packed value of 0.64. The second dimensionless parameter, Φ, is given by:

$$\Phi = \frac{\phi_0}{\phi_p - \phi_0} \qquad \text{Eq. 3}$$

where $\phi_0$ is the particle volume fraction in the bulk suspension (here, $\phi_0$ = 0.05). Dendritic structures are predicted when $D/(1 + \Phi) > 1$, whereas lensing regimes are predicted when this value is less than one. Thus, transitions from dendritic to lensing regimes are predicted as the solidification velocity decreases, or with increases in thermal gradient, particle volume fraction, or particle radius (here, $G$, $\phi_0$, and $r$ are held constant, while $V$ is varied from 6.5 to 80 $\mu m \cdot s^{-1}$).

The microstructures for all translation velocities explored here are predicted to be within the lensing regime. Inconsistent with model predictions, anisotropic, directional lamellar structures are observed for $V$ = 38 and 80 $\mu m \cdot s^{-1}$. This model does not account for solute effects; the dispersant used in our suspensions likely contributed to the breakdown of the solid/liquid interface [36] and may have promoted the development of anisotropic structures outside model predictions. At $V$ = 6.5 $\mu m \cdot s^{-1}$, a transition between dendritic to lensing microstructures is observed from the outer to inner region of the samples. The transition to lensing with decreasing $V$ is qualitatively consistent with this model, but it is notable that lensing is observed in the central regions of samples *only*; this observation may be attributable to convective effects [29], which are also not accounted for in the model. We described similar observations previously for directional solidification of aqueous $TiO_2$ suspensions [29], wherein macroscopic curvature of the solid/liquid interface (resulting from convection) leads to radial variation in particle wall width (dependent on distance from the center) and banding in the central regions of samples; as described earlier, we attributed

banding to particle build-up within the central region of samples from both the interface curvature itself as well as convective mixing in the bulk liquid (ahead of the interface).

## 4. Conclusions

To investigate the suitability of naphthalene as a suspending fluid for freeze-casting applications, suspensions of 5 vol.% (32 wt.%) Cu microparticles in naphthalene, sterically stabilized by the polymeric surfactant Hypermer KD-13 (1 wt.% with respect to Cu particle mass), were directionally solidified in a Bridgman furnace at translation velocities, $V$ = 6.5, 38, and 80 $\mu m \cdot s^{-1}$. The following main conclusions are drawn:

1. Directional microstructures are predominantly observed, comprising colonies of nearly particle-free naphthalene lamellae interspersed with particle-enriched interlamellar regions.
2. At $V$ = 38 and 80 $\mu m \cdot s^{-1}$, a preferred growth direction is observed along the thermal gradient imposed during solidification, over the full height of solidified samples.
3. At $V$ = 6.5 $\mu m \cdot s^{-1}$, a transition from lamellar to lensing microstructures is observed from the regions closest to the ampoule wall to the central regions, suggestive of a macroscopic curvature of the solid/liquid interface during solidification.
4. For all $V$, the thickness of lamellae increases with increasing distance from the region near the ampoule wall (with lamellae thinnest in the central regions of samples) and lamellae show secondary arms on one, not both, of their sides.
5. Both the presence of asymmetric dendritic features and radial variation in lamellar thickness are suggestive of buoyancy-driven convective fluid flow during solidification. As suspensions were solidified in a buoyancy-stable configuration for naphthalene (vertically upward, with denser solid naphthalene below and lighter liquid above), convective fluid

motion is likely introduced due to radial temperature gradients which are often present during Bridgman solidification.

**Acknowledgements**

This work was supported by a grant from NASA's Physical Sciences Research Program (80NSSC18K0196). This research used resources from the MatCI Facility which is supported by the MRSEC program of the National Science Foundation (DMR-1121262) at the Materials Research Center at Northwestern University.

**Declaration of Competing Interest**—DCD discloses a financial interest in Cell Mobility, Inc, a company involved with freeze-casting of metal foams.

**Data availability**—the datasets generated during and/or analyzed during the current study are available from the corresponding author on request.

**References**

[1] K. Scotti, D. Dunand, Freeze casting - A review of processing, microstructure and properties via the open data repository, FreezeCasting.net, Prog. Mater. Sci. 94 (2018) 243-305.
[2] S. Deville, Freeze-casting of porous ceramics: A review of current achievements and issues, Adv. Eng. Mater. 10(3) (2008) 155-169.
[3] U. Wegst, M. Schecter, A. Donius, P. Hunger, Biomaterials by freeze casting, Philos. Trans. R. Soc. 368(1917) (2010) 2099-2121.
[4] S. Wilke, D. Dunand, Structural evolution of directionally freeze-cast iron foams during oxidation/reduction cycles, Acta Mater. 162 (2019) 90-102.
[5] D. Ghosh, N. Dhavale, M. Banda, H. Kang, A comparison of microstructure and uniaxial compressive response of ice-templated alumina scaffolds fabricated from two different particle sizes, Ceram. Int. 42(14) (2016) 16138-16147.
[6] K. Yan, F. Xu, S. Li, Y. Li, Y. Chen, D. Wang, Ice-templating of chitosan/agarose porous composite hydrogel with adjustable water-sensitive shape memory property and multi-staged degradation performance, Colloid Surface B (2020) 110907.
[7] S. Deville, E. Saiz, A. Tomsia, Ice-templated porous alumina structures, Acta Mater. 55(6) (2007) 1965-1974.
[8] C. Pekor, B. Groth, I. Nettleship, The effect of polyvinyl alcohol on the microstructure and permeability of freeze-cast alumina, J. Am. Ceram. Soc 93(1) (2010) 115-120.

[9] S. Miller, X. Xiao, K. Faber, Freeze-cast alumina pore networks: Effects of freezing conditions and dispersion medium, J. Eur. Ceram. Soc. 35(13) (2015) 3595-3605.
[10] H. Choi, T. Yang, S. Yoon, B. Kim, H. Park, Porous alumina/zirconia layered composites with unidirectional pore channels processed using a tertiary-butyl alcohol-based freeze casting, Mater. Chem. Phys. 133(1) (2012) 16-20.
[11] K. Araki, J.W. Halloran, Room-temperature freeze casting for ceramics with nonaqueous sublimable vehicles in the naphthalene-camphor eutectic system, J. Am. Ceram. Soc 87(11) (2004) 2014-2019.
[12] L. Lacerda, D.F. Souza, E. Nunes, M. Houmard, Macroporous alumina structures tailored by freeze-casting using naphthalene-camphor as freezing vehicle, Ceram. Int. (2018).
[13] S. Oh, Y. Do-Kim, M. Suk, Freeze drying for porous Mo with different sublimable vehicle compositions in the camphor-naphthalene system, Mater. Lett. 139 (2015) 268-270.
[14] L. Fabietti, R. Trivedi, Nonequilibrium effects during the ledgewise growth of a solid-liquid interface, Metall Trans A 22 (1991) 1249-1258.
[15] N. Djordjevic, Solubilities of polycyclic aromatic hydrocarbon solids in n-octadecane, Thermochim. Acta 177 (1991) 109-118.
[16] M. Asuncion, J. Goh, S. Toh, Anisotropic silk fibroin/gelatin scaffolds from unidirectional freezing, Mater. Sci. Eng. C 67 (2016) 646-656.
[17] J. Weaver, S. Kalidindi, U. Wegst, Structure-processing correlations and mechanical properties in freeze-cast Ti-6Al-4V with highly aligned porosity and a lightweight Ti-6Al-4V-PMMA composite with excellent energy absorption capability, Acta Mater. (2017).
[18] C.E. Chang, W.R. Wilcox, Localized interface breakdown in zone melting and the travelling heater method, J. Cryst. Growth 21(2) (1974) 182-186.
[19] V. De Leeuw, W. Poot, T.W. De Loos, J. de Swaan Arons, High pressure phase equilibria of the binary systems N2+ benzene, N2+ p-xylene and N2+ naphthalene, Fluid Phase Equilibr. 49 (1989) 75-101.
[20] L. Fabietti, R. Trivedi, In situ observations of stress-induced defect formation at the solid—liquid interface, J. Cryst. Growth 173(3-4) (1997) 503-512.
[21] W. Gao, K. Gasem, R. Robinson, Solubilities of nitrogen in selected naphthenic and aromatic hydrocarbons at temperatures from 344 to 433 K and pressures to 22.8 MPa, J. Chem. Eng. Data 44(2) (1999) 185-189.
[22] D. Olness, H. Sponer, Phosphorescence lifetime studies in some organic crystals at low temperatures, J. Chem. Phys. 38(7) (1963) 1779-1782.
[23] J. Schindelin, I. Arganda-Carreras, E. Frise, V. Kaynig, M. Longair, T. Pietzsch, S. Preibisch, C. Rueden, S. Saalfeld, B. Schmid, Fiji: an open-source platform for biological-image analysis, Nat. Methods 9(7) (2012) 676-682.
[24] L. Fabietti, R. Trivedi, Nonequilibrium effects during the ledgewise growth of a solid-liquid interface, Metallurgical Transactions A 22 (1991) 1249-1258.
[25] L.M. Fabietti, R. Trivedi, In situ observations of stress-induced defect formation at the solid—liquid interface, Journal of crystal growth 173(3-4) (1997) 503-512.
[26] L. Fabietti, R. Trivedi, Nonequilibrium effects during the ledgewise growth of a solid-liquid interface, Metallurgical Transactions A 22(6) (1991) 1249-1258.
[27] J. Deschamps, M. Georgelin, A. Pocheau, Crystal anisotropy and growth directions in directional solidification, Europhysics Letters 76(2) (2006) 291-297.

[28] N. Zabaras, T. Nguyen, Control of the freezing interface morphology in solidification processes in the presence of natural convection, International Journal for Numerical Methods in Engineering 38(9) (1995) 1555-1578.
[29] K. Scotti, L. Kearney, J. Burns, M. Ocana, L. Duros, A. Shelhamer, D. Dunand, The effect of solidification direction with respect to gravity on ice-templated TiO2 microstructures, J. European Ceram. Soc. 39(10) (2019) 3180-3193.
[30] F. Cao, F. Yang, H. Kang, C. Zou, T. Xiao, W. Huang, T. Wang, Effect of traveling magnetic field on solute distribution and dendritic growth in unidirectionally solidifying Sn–50wt% Pb alloy: An in situ observation, J. Cryst. Growth 450 (2016) 91-95.
[31] J. You, Z. Wang, M. Worster, Controls on microstructural features during solidification of colloidal suspensions, Acta Mater. 157 (2018) 288-297.
[32] F. Mota, K. Ji, L.S. Littles, R. Trivedi, A. Karma, N. Bergeon, Influence of macroscopic interface curvature on dendritic patterns during directional solidification of bulk samples: Experimental and phase-field studies, Acta Materialia 250 (2023) 118849.
[33] G. Della Gatta, M. Richardson, S. Sarge, S. Stølen, Standards, calibration, and guidelines in microcalorimetry. Part 2. Calibration standards for differential scanning calorimetry*(IUPAC Technical Report), Pure Appl. Chem. 78(7) (2006) 1455-1476.
[34] A. Campbell, The system naphthalene-benzene considered as an ideal solution Can J Res 19(6) (1941) 143-149.
[35] G. Davis, R. Porter, Application of the differential scanning calorimeter to purity measurements, J. Therm. Anal. Calorim. 1(4) (1969) 449-458.
[36] J.D. Hunt, Pattern formation in solidification, Mater. Sci. Technol. 15(1) (1999) 9-14.

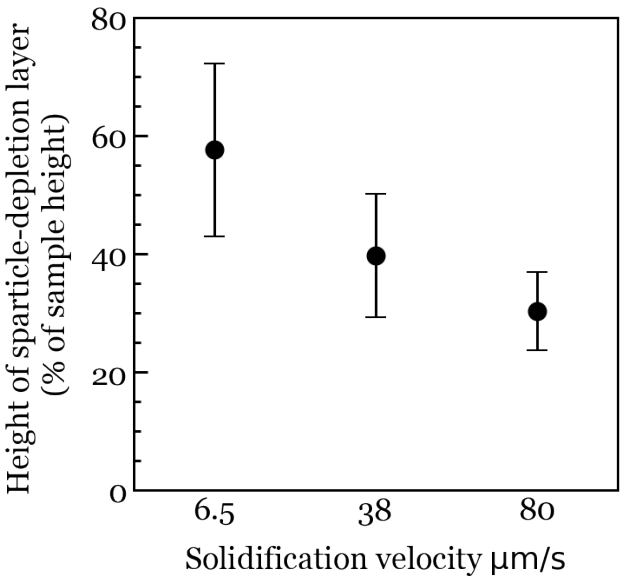


Fig. 1. Plot of particle depletion layer height (as a percentage of total sample height of ~20 cm) vs. solidification velocity for naphthalene/Cu particle suspensions stabilized with Hypermer KD13. Error bars represent standard deviation.

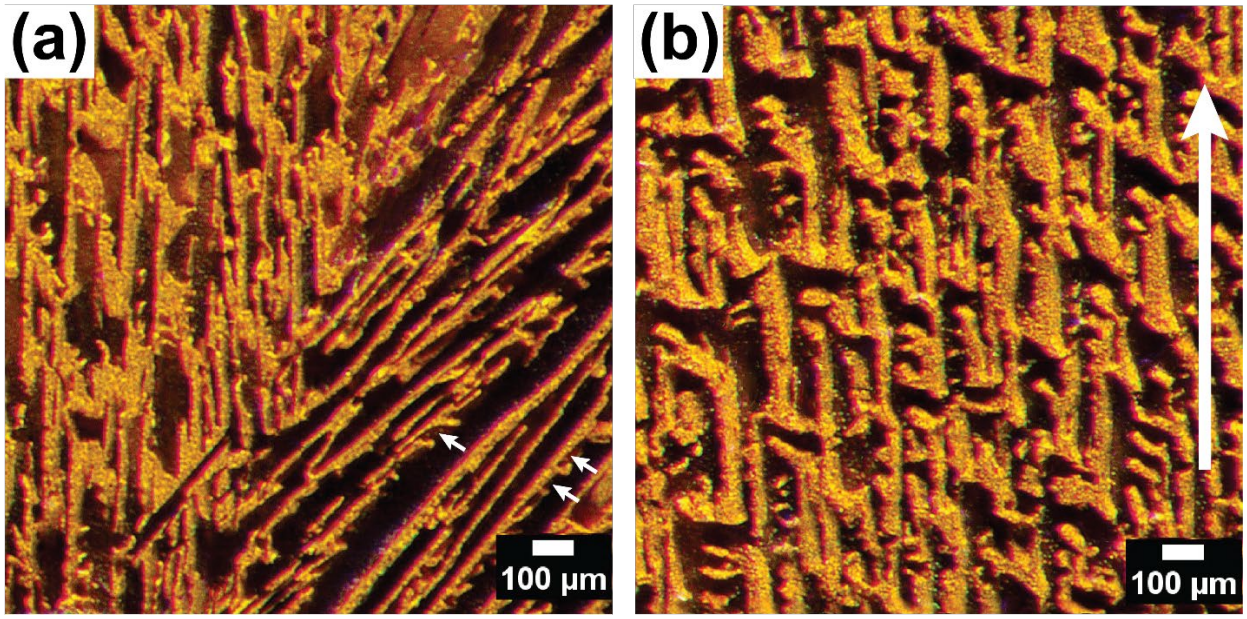


Fig. 2. Optical micrographs of naphthalene/Cu particle suspensions directionally solidified under the fastest translation velocity studied ($V = 80\ \mu m \cdot s^{-1}$), where cross-sections (a) and (b) are taken perpendicular and parallel to the freezing direction, respectively; the large white arrow in (b) shows the freezing direction. Naphthalene lamellae show as dark regions and copper particle-packed interlamellar regions have a golden color; asymmetric secondary arms in naphthalene are highlighted with small white arrows in (a).

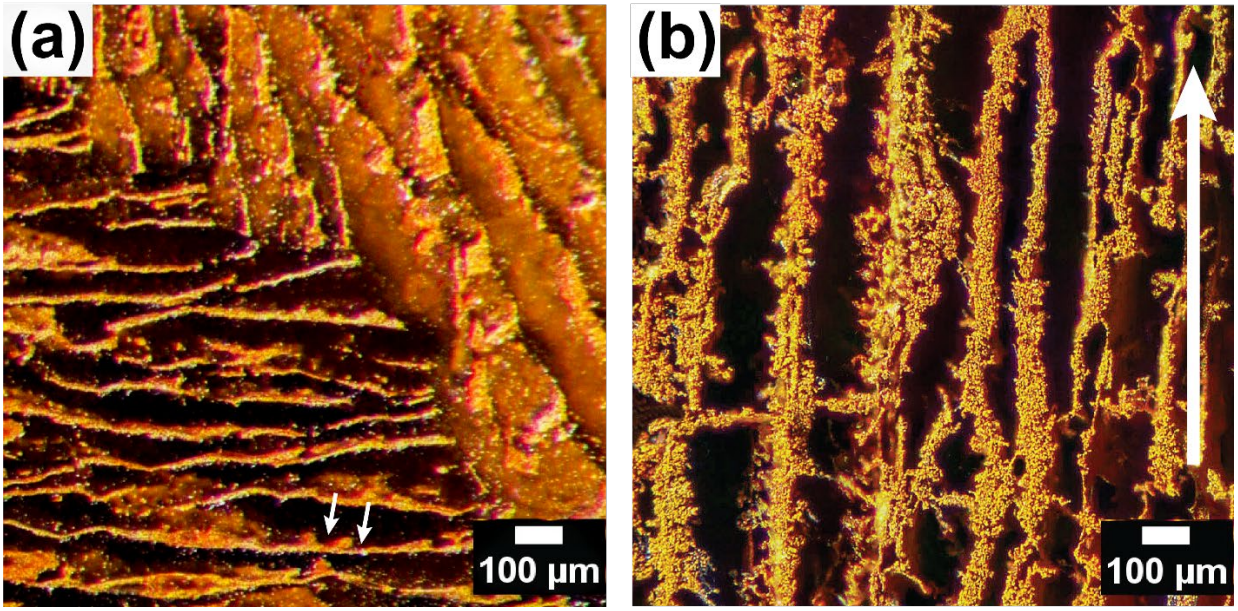


Fig. 3. Optical micrographs of naphthalene/Cu particle suspensions directionally solidified under the intermediate translation velocity studied ($V = 38\ \mu m \cdot s^{-1}$), where cross-sections (a) and (b) were taken perpendicular and parallel to the freezing direction, respectively; the large white arrow in (b) shows the freezing direction. Macro-regions of naphthalene show as dark regions in these images; copper particle-packed walls are golden in color. Asymmetric secondary arm growth of naphthalene is highlighted with small white arrows in (a).

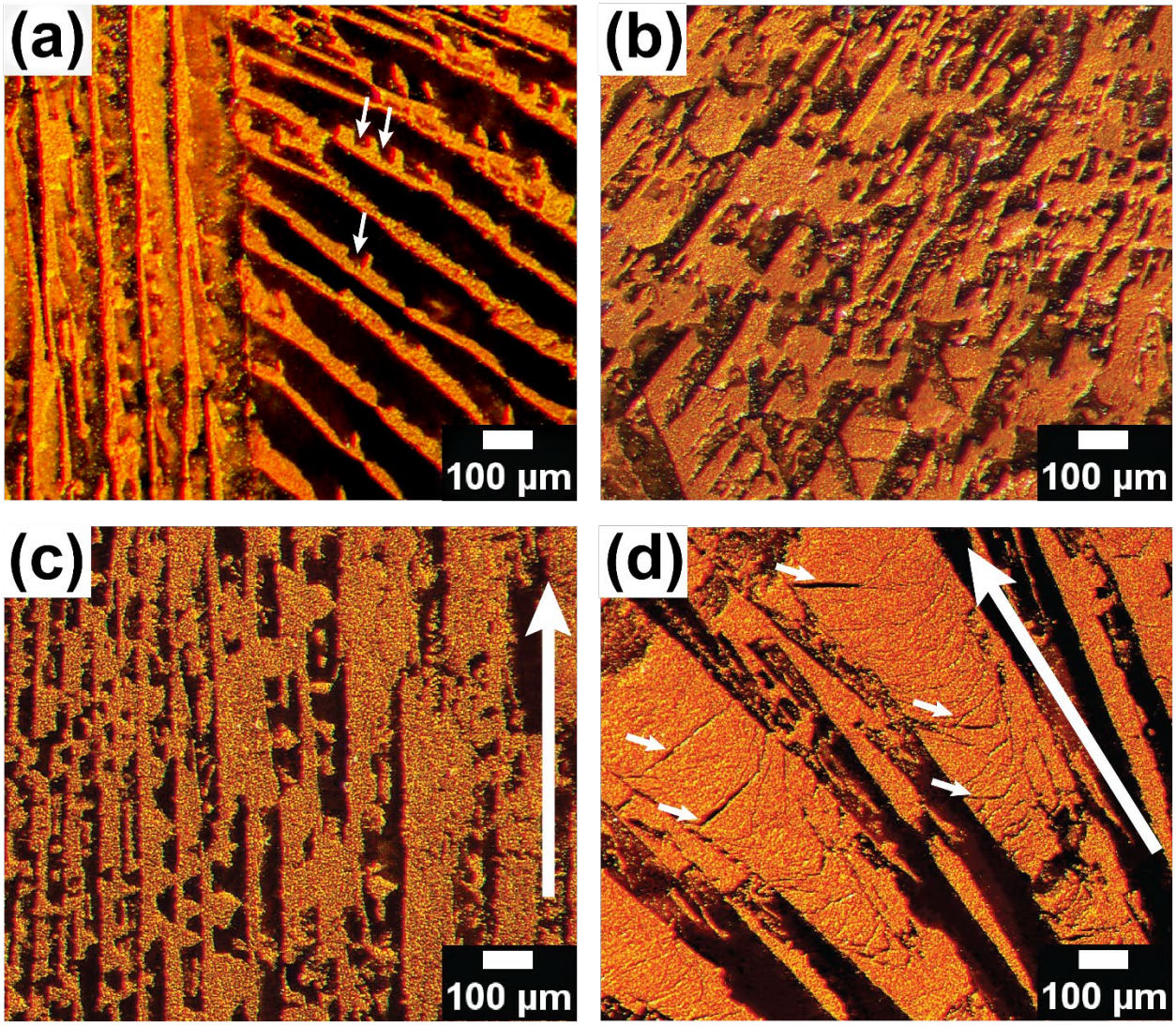


Fig. 4. Optical micrographs of naphthalene/Cu particle suspensions directionally solidified under the slowest translation velocity studied ($V = 6.5\ \mu m \cdot s^{-1}$), where cross-sections (a, b) were taken perpendicular to the freezing direction and (c, d) were taken parallel to the freezing direction (the large white arrows in (c, d) show the freezing direction). Images (a) and (c) were taken from the outer regions of samples (closest to the ampoule wall) whereas (b) and (d) were taken from central regions. Macro-regions of naphthalene show as dark regions in these images; copper particle-packed walls are golden in color; asymmetric dendritic features (a) and banding defects (d) are marked with small white arrows.

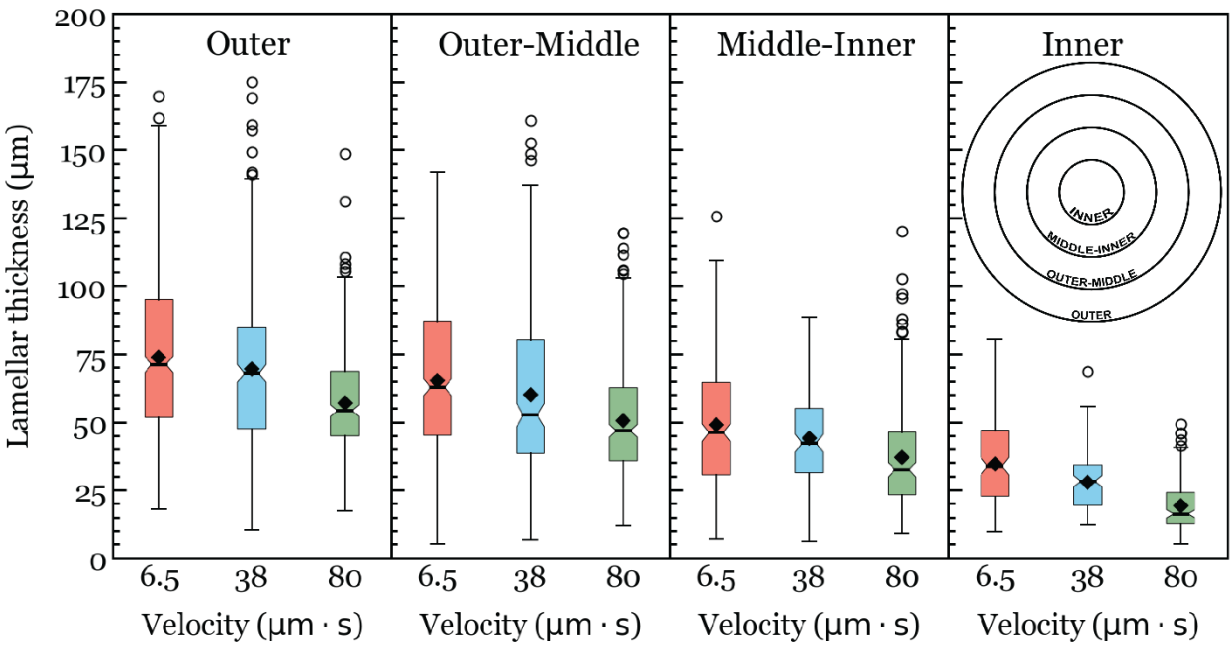


Fig. 5. Box and whisker plots summarizing thickness of naphthalene lamellae in sterically-stabilized naphthalene/Cu particle suspensions after directionally solidification using furnace translation velocities, $V$ = 6.5, 38, and 80 μm · $s^{-1}$. "Outer", "outer-middle", "middle-inner" and "inner" measurements are described in text and illustrated in insert. The minimum and maximum values of boxes represent the first and third quartiles, respectively; medians are shown as horizontal lines inside the boxes, means are represented by black diamonds, and whiskers represent 1.5 times the interquartile range.

Table 1. Thickness of naphthalene lamellae in suspensions of Cu microparticles that were directionally solidified at furnace translation velocities of 6.5, 38, and 80 μm · $s^{-1}$. All measurements were taken from cross-sections perpendicular to the freezing directions, with "outer", "outer-middle", "middle-inner" and "inner" measurements obtained from equally spaced regions, as described in text and shown in the insert of Fig. 5. Data are expressed as mean ± standard deviation; $N$ is the number of samples.

| Velocity (μm · $s^{-1}$) | $N$ | Naphthalene lamellae thickness (μm) | | | |
|---|---|---|---|---|---|
| | | Outer | Outer-middle | Middle-inner | Inner |
| 6.5 | 3 | 73±31 | 65±28 | 49±23 | 36±15 |
| 38 | 3 | 69±29 | 60±31 | 44±17 | 28±10 |
| 80 | 3 | 57±19 | 50±21 | 37±20 | 19±10 |

Professor Ramamoorthy Ramesh
Editor in Chief
Journal of Materials Research

August 1, 2023

Dear Ramamoorthy,

I would like to submit to Journal of Materials Research a full-length article entitled, “Lamellar structures in directionally solidified naphthalene suspensions” written by Peter Voorhees, David Dunand, and myself.

In this manuscript, we investigate naphthalene as a suspending fluid for freeze-casting applications. The freeze-casting solidification technique has been used extensively for over a decade for the fabrication of porous materials, and naphthalene has only been tested as part of a fluid system (with camphor). Previous reports show resulting structures that were disordered. Here, we demonstrate anisotropic, directional structures using only naphthalene as the suspending fluid by solidifying suspensions using a Bridgman furnace (which offers more control over the thermal gradient relative to traditional freeze-casting set-ups).

We believe that this manuscript is a good fit for Journal of Materials Research given the high activity in the field. This manuscript should be of interest to a broad readership, including those interested in general solidification techniques, biomaterials, geology, and porous ceramic, polymeric and metallic materials processing, in addition to the freeze-casting community.

This manuscript has not been published and is not under consideration for publication elsewhere, and Journal of the European Ceramic Society is our first choice.

Should the paper be selected and sent for review, knowledgeable reviewers include:
G. Worster (mgw1@cam.ac.uk)
U. Wegst (urlike.wegst@dartmouth.edu)
S. Deville (sdeville@gmail.com)

We are not interacting with these scientists, but we are aware of their extensive knowledge of the freeze-casting technique as they have written previous reviews on the topic.

Thank you for your consideration.

Best regards,

Kristen Scotti